Malaysian Journal of Chemistry, 2026, Vol. 28(2), 319-328
(Special Issue: *1st International Conference on Chemical and Energy Engineering 2025, ICChEE2025*)

Synthesis and Characterization of Iron-Based Additive and Its Impact on Biohydrogen Production

Ahmad Syahmi Mohamed Latiff[1,2], Pua Fei-ling[2,3]*, Siti Zulaikha Nafsun[1,2] and Tan Ee Sann[2,3]
[1]College of Graduate Studies, Universiti Tenaga Nasional, 43000 Kajang, Selangor, Malaysia
[2]Institute of Sustainable Energy (ISE), Universiti Tenaga Nasional, 43000 Kajang, Selangor, Malaysia
[3]Department of Mechanical Engineering, College of Engineering, Universiti Tenaga Nasional, 43000 Kajang, Selangor, Malaysia
*Corresponding author (e-mail: gracepua@uniten.edu.my)

Current renewable energy research focuses on developing environmentally friendly alternatives to fossil fuels, such as solar, wind, geothermal power, and biomass, to reduce greenhouse gas emissions and pollution. Biohydrogen production involves the use of biological processes to generate a clean and efficient energy carrier in the form of hydrogen gas. In this study, an iron-based additive (SC1) was synthesized, and its performance in biohydrogen production was evaluated. The additive was prepared using the hydrothermal method and subsequently tested in a dark fermentation reaction. Raw palm oil mill effluent (POME) was used as the inoculum, with glucose as the substrate. The morphology and elemental composition were characterized by scanning electron microscopy (SEM) and energy-dispersive X-ray spectroscopy (EDX). The structural properties were characterized by X-ray diffraction (XRD). The results revealed that the additive consisted primarily of iron(III) oxyhydroxide and hydrated iron(III) oxide. SEM analysis revealed a porous surface morphology, while EDX confirmed the elemental composition of the material. XRD analysis demonstrated that the additive comprised nanoparticles (NPs) with an average crystallite size of 23.02 nm. The additive performance results showed that under optimized reaction conditions (300 mg/L additive, pH 6, and 37 °C), the biohydrogen yield increased by 7.39% compared to the control experiment. This improvement was likely attributed to enhanced electron transfer and hydrogen-producing bacteria (HPB) enrichment, which increased hydrogenase activity. The study provides evidence that iron-based NPs additives can serve as effective and practical additives in biohydrogen production.

Keywords: Iron-based additive, biohydrogen, hydrothermal, dark fermentation

Received: July 2025; Accepted: January 2026

The global search for sustainable and renewable energy alternatives has intensified due to increasing concerns regarding environmental pollution, climate change, and the depletion of fossil fuels worldwide. In this context, hydrogen's high energy content, and environmental friendliness, with water as the only byproduct, have made it an emerging alternative to fossil fuels [1, 2]. This makes hydrogen a clean energy source that could significantly reduce environmental problems while addressing urgent energy demands. Among the various methods for producing hydrogen, dark fermentation presents a viable and promising strategy for generating hydrogen through biological processes. This method utilizes an anaerobic process that converts diverse organic substrates, such as industrial wastewaters and agricultural residues, into biohydrogen through microbial metabolism [3].

Dark fermentation offers an eco-friendly alternative to fossil fuels [4, 5], and presents numerous advantages; however, its practical application faces significant challenges, including low hydrogen yields, process instability, inadequate microbial activity, nutrient imbalances, and inhibition by metabolic byproducts [4, 5]. To address these limitations and enhance performance, recent studies have investigated the incorporation of metal-based catalysts and additives, specifically iron-based catalysts, to improve hydrogen production and process stability [5]. In microbial metabolism, iron is a vital trace element involved in enzymatic reactions, particularly those catalyzed by hydrogenases and ferredoxins, which play crucial roles in the hydrogen production pathway [6].

Iron-based materials, including iron oxides (FeO_3, FeO_4), zero-valent iron (ZVI), and iron nanoparticles, have demonstrated promise in increasing hydrogen yields through modifying metabolic pathways, boosting electron transfer, and enhancing microbial activity [7, 8, 9]. Furthermore, these iron-based substances can enhance hydrogen selectivity by suppressing competing methanogenic pathways, thereby improving the overall efficiency

†Paper presented at the 1st International Conference on Chemical and Energy Engineering 2025 (ICChEE2025)

of biohydrogen production. Iron-based catalysts improve dark fermentation systems because of their affordability, environmental compatibility, and effectiveness in increasing hydrogen yields [10]. Nevertheless, comprehensive investigation is required to understand the optimal operational conditions, long-term stability, and microbial interactions associated with their application.

According to previous research, iron-based additives have demonstrated significant potential to enhance hydrogen yield production by improving electron transfer pathways, facilitating microbial metabolism, and serving as cofactors for hydrogenase enzymes [11, 12]. Despite these advantages, the mechanisms underlying the effects of various iron-based compounds, including ferrous ions, zero-valent iron, and iron oxides, remain poorly understood. Comparative studies addressing their effectiveness, optimal dosage, and long-term effects on microbial communities and system stability are lacking. This knowledge gap impedes the development of efficient, scalable, and cost-effective biohydrogen production technologies. Therefore, further investigation and optimization are necessary to identify the optimal types, concentrations, and modes of action of these additives.

When optimizing biohydrogen production, iron additives are essential, particularly in microbial processes involving bacteria and algae. These microorganisms generate hydrogen through enzymatic pathways, many of which require iron for optimal catalytic function. Notably, iron is integral to hydrogenase enzyme function, enhancing their catalytic activity and enabling efficient hydrogen production and uptake [13]. The activity of these enzymes can be increased by adding iron compounds to the production system, such as iron sulphate ($FeSO_4$) or iron chloride ($FeCl_3$) [7]. By enhancing microbial metabolism and energy transfer efficiency, microorganisms can produce greater quantities of hydrogen. Iron has been demonstrated to increase hydrogen production in dark fermentation, where bacteria decompose organic matter anaerobically, promoting bacterial growth and metabolic activity [6]. Iron is also essential in photosynthetic fermentation processes, supporting light-dependent energy conversion and hydrogen production by photosynthetic bacteria.

To produce iron-based catalysts capable of enhancing biohydrogen production, hydrothermal synthesis is a popular and effective method. This technique involves employing high-pressure and high-temperature aqueous environments to synthesize materials with unique properties. In the context of biohydrogen production, hydrothermal synthesis is particularly useful for creating iron-based catalysts that enhance the efficiency of microbial hydrogen production processes. Hydrothermal synthesis enables precise control of catalyst properties, such as specific surface area, particle size, and chemical composition, to maximize catalytic activity and stability in hydrogen production [14].

In the past decade, several reviews have emphasized dark fermentation as a robust route for converting diverse organic wastes into hydrogen, yet consistently report a low yield, process instability, and scale-up limitations as major bottlenecks. Recent studies on iron-based additives and nanoparticles (Fe, Fe_3O_4, Fe_2O_3 and bimetallic Ni/Fe systems) have shown hydrogen yield improvements ranging roughly from 20% up to more than two-fold by enhancing electron transfer and activating key enzymes such as hydrogenases and ferredoxins [15, 16]. However, most of these investigations focus on synthetic substrates, short-term batch tests, or single iron species, and often lack systematic evaluation of optimal dosage, long-term stability, and microbial community responses, particularly when applied to complex waste streams like POME sludge. Moreover, while nanomaterial-based strategies have attracted attention, the controlled hydrothermal synthesis of tailored iron-based catalysts specifically designed for dark fermentation and tested on real industrial residues remains underexplored. In this study, these gaps were addressed by developing a hydrothermally synthesized iron-based additive and evaluating its effect on hydrogen yield, process performance, and sludge conversion during dark fermentation of raw POME sludge. The characteristics of the additive were examined and analysed using instrumental characterization technologies.

EXPERIMENTAL

Chemicals and Materials

Ferric sulphate hydrate, $Fe_2(SO_4)_3 \cdot xH_2O$ (>73.0%), and ferrous sulphate heptahydrate, $FeSO_4 \cdot 7H_2O$ (>99.5%), were used in this study. Both chemicals were purchased from Suria Umum Sdn. Bhd. (Malaysia) and Evergreen Engineering & Resources (Malaysia), respectively. D+Glucose anhydrous was purchased from e-Scientific. Raw palm oil mill effluent (POME) sludge was collected from Seri Morib Palm Oil Mill Sdn. Bhd., a local palm oil mill located in Banting, Selangor, Malaysia. The collected POME sludge was stored in a chiller for subsequent use. All materials were used as received.

Characterization Methods

Scanning electron microscopy (SEM) equipped with energy dispersive X-ray (EDX) are used to examine the surface structure and elemental composition. X-ray diffraction (XRD) test is to study the phase identification, crystal orientation, and microstructural characteristics of the materials. The morphology and elemental compositions of SC1 additive was examined by scanning electron microscopy (SEM)

equipped with electron dispersive X-ray spectroscopy (EDX) (JSM-6010PLUS/LV, JEOL, Japan) in Universiti Tenaga Nasional (UNITEN). X-ray diffraction (XRD) investigation was carried out using Bruker's D8 ADVANCE in Centre for Research and Instrumentation Management (i-CRIM), Universiti Kebangsaan Malaysia (UKM), with Cu Kα radiation ($\lambda = 0.154$ nm) in the scanning range (2θ) of 10^0 - 90^0. The phase identification and crystallite size of crystalline later obtained by analysing the graph using DIFFRAC.SUITE software in i-CRIM laboratory, Universiti Kebangsaan Malaysia (UKM).

Preparation of Iron-based Additive

The iron-based additive in this study was prepared through hydrothermal synthesis. Ferric sulphate hydrate, $Fe_2(SO_4)_3 \cdot xH_2O$, and ferrous sulphate heptahydrate, $FeSO_4 \cdot 7H_2O$, were used as precursor materials. First, 0.02 mol of $Fe_2(SO_4)_3 \cdot xH_2O$ and 0.01 mol of $FeSO_4 \cdot 7H_2O$ were dissolved in 300 mL of distilled water. The mixture was stirred homogeneously at 500 rpm in a sealed hydrothermal reactor. The sealed vessel was heated to 185 °C for 16 hours to allow the reaction to proceed. After the reactor cooled to room temperature, the sample was recovered. The precipitate was collected by filtration, and the solid product was oven-dried overnight. The dried sample was then collected and stored in a desiccator for subsequent use. The prepared iron-based additive is denoted as SC1. Figure 1 illustrates the preparation procedure for the iron-based additive. The synthesis process was iteratively optimized: if the SC1 additive produced low hydrogen yield in initial testing, the hydrothermal synthesis was repeated with modified parameters until the desired high hydrogen yield was achieved, as the objective of this study was to develop an iron-based additive using direct hydrothermal synthesis tailored specifically for biohydrogen production.

Effect of Iron-based additive in Biohydrogen Production

The performance of the SC1 additive was evaluated through dark fermentation experiments to assess biohydrogen production. The effect of SC1 on hydrogen (H_2) production was investigated using batch-mode experiments. Anhydrous glucose served as the substrate, while raw POME sludge was used as the inoculum for fermentation. The experiment was conducted in a 500 mL glass bottle containing 200 mL of working volume, filled with raw POME sludge and anhydrous glucose at a concentration of 10 g/L [17, 18]. No additional nutrients were added, as glucose provided a rich carbon source necessary for bacterial growth. Based on previous studies [11], an optimal concentration of 300 mg/L of SC1 additive was added for comparison [11]. The initial pH of each sample was set to 6.0. The bottles were sealed with rubber stoppers and purged with nitrogen gas for 2 minutes to maintain an anaerobic environment. All bottles were placed in an incubator and incubated at 37 °C for 5 days. At regular intervals, gas samples were collected using a syringe for biogas composition analysis by gas chromatography (GC). A gas chromatography system (MicroGC, Agilent) equipped with two channels was used to analyse the biogas produced during the fermentation process. The first channel was equipped with an MS5A SS column (10 m × 0.25 mm × 30 μm), and the second channel was equipped with a PORAPLOT U FS column (10 m × 0.25 mm × 8 μm). Both columns were maintained at 80 °C, and the injectors were set to 90 °C. The pressure settings for Channels 1 and 2 were 200 kPa and 150 kPa, respectively.

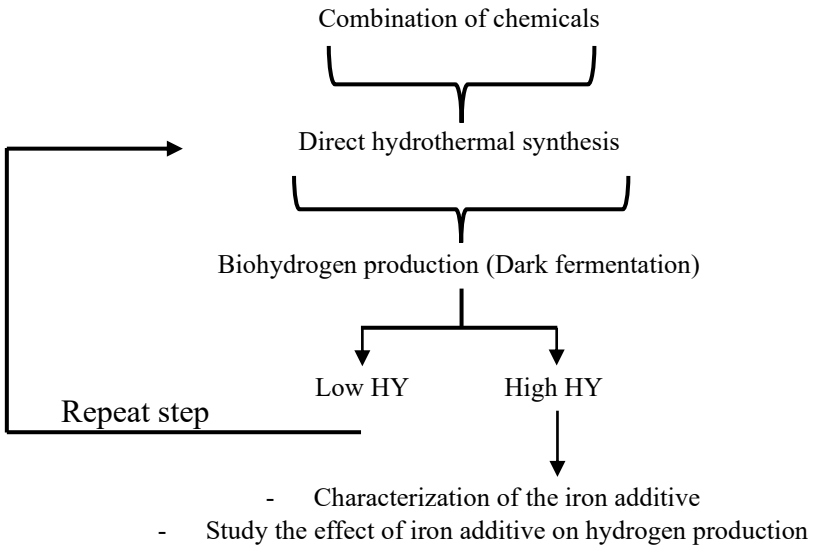

Figure 1. Preparation of iron-based additive.

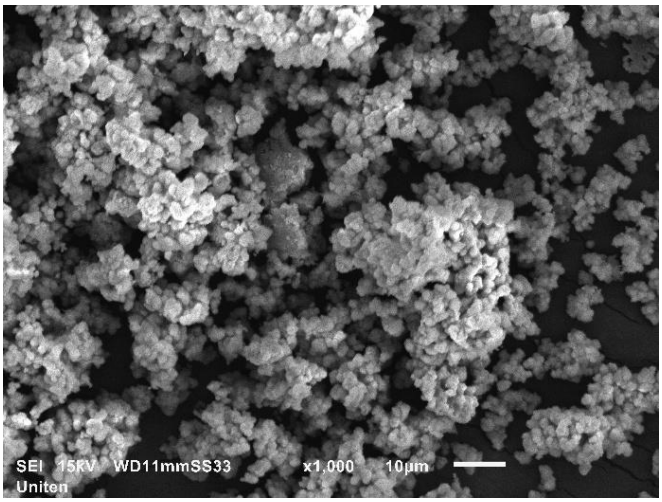

Figure 2. SEM image of SC1 additive.

RESULTS AND DISCUSSION

Characterization of Iron-based Additive

The morphology of SC1 was examined in detail by scanning electron microscopy (SEM), and the results are presented in Figure 2. SEM analysis revealed several key characteristics, including porosity and agglomerated particles within the structure. These observations indicate that the material underwent partial agglomeration during synthesis. Additionally, the morphology consisted predominantly of spherical shapes, suggesting that nanostructured material in the form of nanospheres was successfully produced [19]. he presence of these nanospheres indicates that the material possesses unique surface-area properties and enhanced reactivity, characteristics typically associated with nanomaterials. The observed porosity also suggests the potential for improved performance in applications requiring large specific surface areas, such as catalysis [20].

The elemental composition of SC1 was analysed by energy dispersive X-ray (EDX) and the results are summarised in Table 1. EDX analysis revealed high atomic ratios of iron (Fe) at 29.74% and oxygen (O) at 54.95%, confirming that the intended iron-based compound was successfully synthesized and demonstrating the efficiency of the synthesis process [21]. The predominance of these elements indicates that the primary chemical components were well integrated into the final product. In addition to Fe and O, minor elements unrelated to the parent reactants were also detected. These elements are likely attributable to trace impurities introduced during the synthesis process, possibly from laboratory handling, residual precursor materials, or contamination during the hydrothermal synthesis. Such minor impurities are common in nanomaterial synthesis and are generally unavoidable under standard experimental conditions.

Table 1. Elemental compositions of SC1 additive.

Element	Weight%	Atomic%
Iron (Fe)	47.07	29.74
Oxygen (O)	24.92	54.95
Chromium (Cr)	8.83	5.99
Zirconium (Zr)	7.71	2.98
Terbium (Tb)	6.53	1.45
Sulphur (S)	3.84	4.22
Nickel (Ni)	1.11	0.67

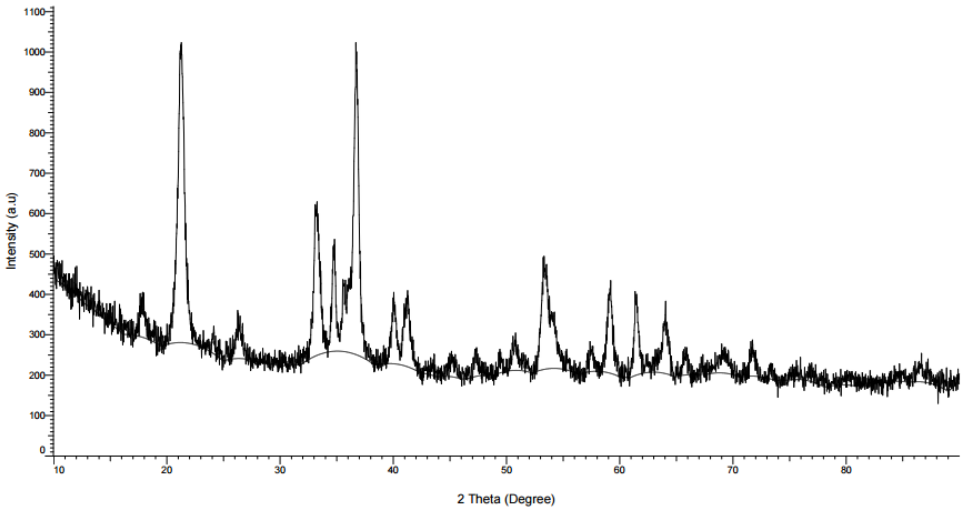

Figure 3. XRD pattern of SC1 additive.

X-ray diffraction (XRD) analysis of SC1 was performed to investigate the crystalline structure of the additive, and the corresponding results are presented in Figure 3. As shown in Figure 3, the SC1 XRD pattern exhibits broad diffraction peaks in the 2θ range of 20° to 80°, which is typical of low-crystallinity materials. The presence of these broadened peaks indicates that SC1 comprises nanocrystalline and partially amorphous structures, since peak broadening is typically associated with reduced crystalline size and structural defects. Further analysis of the diffraction pattern reveals that SC1 consists of approximately 74.5% crystalline phase and 25.5% amorphous phase. This mixed-phase composition confirms the coexistence of ordered crystalline and disordered amorphous regions in the material, which is characteristic of nanostructured materials synthesized under hydrothermal or similar conditions.

The crystallite sizes at various peaks were measured and presented in Table 2. The average particle diameter (D) was obtained from the main diffraction peaks using Scherrer's formula: $D = K\lambda/(\beta \cos\theta)$, where λ is the wavelength (Cu Kα), K is the shape factor constant, β is the full width at half-maximum (FWHM), and θ is the Bragg diffraction angle. The average crystallite size of SC1 calculated from multiple diffraction peaks using standard XRD was found to be approximately 23.02 nm, confirming that the material is nanoscale. Nanosized crystallites promote the formation of nanostructured materials, consistent with the observed peak broadening in the XRD pattern. As shown in Figure 3, the XRD diffraction pattern displays characteristic reflections corresponding to iron(III) oxyhydroxide, $Fe^{+3}O(OH)$ (PDF 00-029-0731), and hydrated iron(III) oxide, $Fe_2O_3 \cdot H_2O$ (PDF 00-008-0097). These diffraction signals indicate that goethite is the predominant crystalline phase in the SC1 compound. The coexistence of these iron-based phases indicates that the synthesis conditions favored the formation of iron-oxyhydroxide structures commonly associated with hydrothermal processes and known for their stability and functional properties.

Table 2. Various peak of SC1 additive and its crystalline size.

Index	Maximum Peak	FWHM	Crystalline Size (nm)
1	21.26	0.64	11.59
2	33.22	0.57	14.39
3	34.76	0.31	34.19
4	36.74	0.46	14.26
5	40.06	0.38	25.81
6	41.27	0.51	15.78
7	53.39	0.96	9.74
8	59.14	0.56	16.97
9	61.45	0.37	25.79

Catalytic Performance of Iron-based Additive

The effect of SC1 on fermentative hydrogen production was systematically investigated during this study. All experimental runs were performed in triplicate to ensure reproducibility and reliability of the results. The cumulative hydrogen volume and hydrogen yield obtained from the control and SC1-enhanced experiments are summarized in Tables 3 and 4. Hydrogen production performance was assessed using two main parameters: hydrogen yield and hydrogen production rate.

Hydrogen and carbon dioxide were identified as the primary gaseous products during anaerobic fermentation of raw palm oil mill effluent (POME) sludge. Trace amounts of methane were occasionally detected during the early sampling phases; however, methane was not observed in later fermentation phases. This observation indicates that minimal methanogenic bacteria were present in the fermentation medium and that their activity was effectively suppressed over time, allowing the dominance of hydrogen-producing pathways.

Hydrogenase plays a key role in hydrogen production and is a rate-limiting enzyme in microbial metabolism. The expression level and catalytic activity of hydrogenase directly affect the metabolic efficiency of hydrogen-producing bacteria (HPB), and consequently, both the hydrogen yield and overall efficiency of hydrogen production are affected. The introduction of SC1 appears to exert a positive effect on microbial activity, possibly by enhancing hydrogenase function or promoting the growth of HPB.

Based on the experimental results, the average hydrogen yield increased by 7.39% with the addition of SC1 compared to the control. This improvement demonstrates that SC1 successfully enhanced the productivity of dark fermentation by stimulating microbial metabolic activity. Additionally, the average biohydrogen production rate - defined as the total hydrogen produced divided by the experiment duration - also improved. As shown in Tables 3 and 4, the mean hydrogen production rates for the control and SC1-enhanced systems were 9.20 mL/day and 9.88 mL/day, respectively, representing a significant increase in hydrogen production with SC1 addition.

Table 3. Value of cumulative H_2 volume and hydrogen yield of control experiment.

Time (days)	C1		C2		C3		Average
	V cum H_2 (mL)	V H_2/g VS	V cum H_2 (mL)	V H_2/g VS	V cum H_2 (mL)	V H_2/g VS	V H_2/g VS
0	0	0	0	0	0	0	0
1	5.46	2.73	4.43	2.22	6.41	3.2	2.72
1	37.95	18.98	37.49	18.75	40.32	20.16	19.29
1	42.46	21.23	44.68	22.34	48.8	24.4	22.66
2	42.46	21.23	45.12	22.56	49.41	24.7	22.83
2	42.77	21.38	45.12	22.56	49.41	24.7	22.88
2	42.82	21.41	45.12	22.56	49.41	24.7	22.89
3	42.82	21.41	45.12	22.56	49.41	24.7	22.89
3	42.82	21.41	45.15	22.57	49.41	24.7	22.9
4	42.82	21.41	45.15	22.57	49.45	24.73	22.9
4	42.82	21.41	45.26	22.63	49.45	24.73	22.92
5	43.02	21.51	45.37	22.68	49.6	24.8	23
5	43.02	21.51	45.37	22.68	49.6	24.8	23

Table 4. Value of cumulative H_2 volume and hydrogen yield of SC1 experiment.

Time (days)	SC1-1		SC1-2		SC1-3		Average
	V cum H_2 (mL)	V H_2/g VS	V cum H_2 (mL)	V H_2/g VS	V cum H_2 (mL)	V H_2/g VS	V H_2/g VS
0	0	0	0	0	0	0	0
1	11.19	5.6	10.21	5.11	14.67	7.33	6.01
1	42.49	21.24	47.65	23.83	46.62	23.31	22.79
1	45.99	23	52.05	26.03	49.84	24.92	24.65
2	45.99	23	52.05	26.03	49.84	24.92	24.65
2	45.99	23	52.05	26.03	49.84	24.92	24.65
2	45.99	23	52.05	26.03	49.84	24.92	24.65
3	45.99	23	52.05	26.03	49.84	24.92	24.65
3	45.99	23	52.05	26.03	49.84	24.92	24.65
4	45.99	23	52.05	26.03	49.84	24.92	24.65
4	45.99	23	52.05	26.03	49.84	24.92	24.65
5	46.17	23.09	52.05	26.03	49.84	24.92	24.68
5	46.17	23.09	52.05	26.03	49.98	24.99	24.7

Figure 4 shows the hydrogen yield averages for the control and SC1 additive during dark fermentation experiments. Figure 4 demonstrates that hydrogen production was minimal in the early hours at a steady rate. After 12 hours, hydrogen production increased more than threefold; however, after 24 hours, the production rate reached its maximum and remained nearly stable for the following days before decreasing on the fifth day. The average hydrogen yield obtained during dark fermentation of POME was 23 V H_2/g VS for the control and 24.7 V H_2/g VS with the SC1 additive. The lower hydrogen content in the biogas is probably attributable to the complexity of raw POME, as reported in previous studies [22, 23]. It can be observed that the production rate and yield of hydrogen improved with the addition of SC1 additive during fermentation. This improvement was likely due to the enrichment of hydrogen-producing bacteria (HPB) and enhanced electron transfer, which increased the activity of hydrogenase [24, 25]. Previous studies found that this improvement resulted from the release of iron (Fe) from Fe_2O_3 nanoparticles during the biohydrogen production process, facilitated by volatile fatty acids (VFAs) [26]. Given that [Ni-Fe] and [Fe-Fe] hydrogenase are the two main types of hydrogenase enzymes, the optimal amount and conditions of iron may supply the necessary elements for bacterial growth and hydrogenase synthesis, thereby enhancing the hydrogen yield [27].

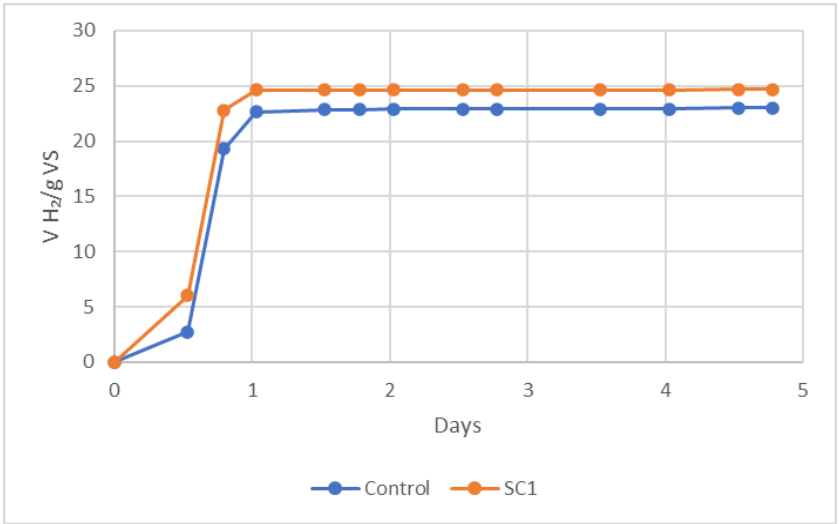

Figure 4. Graph of average hydrogen yield for control and SC1.

Table 5. Comparative of other iron-based additives.

Iron-based additive	Inoculum	Subtract	H_2 yield (%)	References
Fe_2O_3	Enterobacter cloacae 811101	Sucrose	14	[29]
$FeSO_4$	Ethanoligenens harbinense YUAN-3	Glucose	12.60	[30]
$FeCl_2$	Grass composts	Food waste	7.10	[31]
SC1	Raw POME sludge	Glucose anhydrous	7.39	This study

These findings support the hypothesis that adding iron nanoparticles to POME enhances hydrogen productivity by increasing the bioactivity of hydrogen-producing bacteria. Additionally, it was discovered that Fe_2O_3 nanoparticles (NPs) could enhance electron transfer rates by increasing ferredoxin oxidoreductase activity. This enhancement was facilitated by the increased surface area, which boosted hydrogen production during the dark fermentation process [24]. Some researchers have also proposed that NPs function as "bridges" to promote extracellular electron transfer between interconnected HPB cells [28]. Due to the high conductivity of iron nanoparticles, the electron transfer efficiency in hydrogen fermentation can be significantly enhanced at sufficient particle concentrations.

The effect of different iron-based additives on fermentative hydrogen production is illustrated in Table 5. The table compares the performance of iron-based additives in biohydrogen production. The biohydrogen yield obtained in this study was lower than that reported in other studies, primarily because POME contains complex polymers (insoluble materials) that are difficult for microbes to degrade into simpler compounds, such as monomers and oligomers (soluble materials), without pretreatment [32]. It is important to note that the higher hydrogen yields reported in other studies were largely due to additional pretreatment steps applied to the inoculum and substrate prior to dark fermentation. In contrast, this study utilized raw POME sludge and anhydrous glucose without any pretreatment to isolate and evaluate the effectiveness of the SC1 additive without confounding factors. Although the SC1 additive improved biohydrogen production, the overall hydrogen yield remained limited compared to other studies. This limitation is attributed to several factors inherent to the dark fermentation process. Previous studies in dark fermentation processes shows that it is possible to significantly increase hydrogen production with addition of SC1 by optimizing the inoculum through pretreatment and preparing the medium as a substrate, alongside optimizing dark fermentation conditions [18, 23. 33, 34]. Nevertheless, this study is significant because it demonstrates that using raw materials with a simply synthesized SC1 additive can still considerably increase the hydrogen production rate and yield. The bacteria provided by the anaerobic POME sludge interact with the goethite surface (SC1) to facilitate the electron transfer process and thus improve the production of biohydrogen [26]. This underscores the effectiveness of the SC1 additive in enhancing the dark fermentation process independently of other factors. Furthermore, these results suggest that the SC1 additive can improve biohydrogen production while reducing the costs and time associated with raw material preparation, such as culture medium formulation and inoculum treatment.

CONCLUSION

This study developed a methodology to synthesize iron-based additive through hydrothermal reaction process specifically for improving biohydrogen production process. The chemicals combination and parameters for hydrothermal synthesis carefully studied tailored to improve the performance of biohydrogen production. The results of this study demonstrated the production of iron-based additive presented by SC1 which exhibit a good performance in dark fermentation process by increasing 7.39% of the hydrogen yield and 9.88 mL/days hydrogen production rate. In summary, the additive prepared possessed good properties that have potential to be used as an effective, and practical additive in biohydrogen production. These findings demonstrated that adding iron NPs to POME for efficient fermentation improves both the production rate and hydrogen yield. By optimizing the synthesis method of iron-based additive, it can further improve the properties and performance of the additive in assisting the production of hydrogen yield and its rate across various fermentative condition for biohydrogen method.

ACKNOWLEDGEMENTS

The authors want to acknowledge the financial support and facilities provided by UNITEN – AAIBE PROJECT (KETTHA 2023) – Chair of Renewable Energy grant – 202303KETTHA.

REFERENCES

1. Liu, Y., Min, J., Feng, X., He, Y., Liu, J., Wang, Y., He, J., Do, H., Sage, V., Yang, G. and Sun, Y. (2020) A review of biohydrogen productions from lignocellulosic precursor via dark fermentation: Perspective on hydrolysate composition and electron equivalent balance. *Energies*, **13(10)**.

2. Wang, Y., Tang, M., Ling, J., Wang, Y., Liu, Y., Jin, H., He, J. and Sun, Y. (2021) Modeling biohydrogen production using different data driven approaches. *International Journal of Hydrogen Energy*, **46(58)**.

3. Teke, G. M., Anye Cho, B., Bosman, C. E., Mapholi, Z., Zhang, D. and Pott, R. W. M. (2024) Towards industrial biological hydrogen production: a review. *World Journal of Microbiology and Biotechnology*, **40(1)**.

4. Albuquerque, M. M., Sartor, G. de B., Martinez-Burgos, W. J., Scapini, T., Edwiges, T., Soccol, C. R. and Medeiros, A. B. P. (2024) Biohydrogen Produced via Dark Fermentation: A Review. *Methane*, **3(3)**, 500–532.

5. Sohale, A. P., Janardanan, S., Yadav, D., Dash, B. and Yadav, M. D. (2023) Dark Fermentative Biohydrogen Production: Recent Advances and Challenges. *Industrial and Engineering Chemistry Research*, **62(37)**.

6. Ren, Y., Si, B., Liu, Z., Jiang, W. and Zhang, Y. (2022) Promoting dark fermentation for biohydrogen production: Potential roles of iron-based additives. *International Journal of Hydrogen Energy*, **47(3)**, 1499–1515.

7. Liu, Y., Liu, J., He, H., Yang, S., Wang, Y., Hu, J., Jin, H., Cui, T., Yang, G. and Sun, Y. (2021) A review of enhancement of biohydrogen productions by chemical addition using a supervised machine learning method. *Energies*, **14(18)**.

8. Zhu, H., Seto, P. and Parker, W. J. (2014) Enhanced dark fermentative hydrogen production under the effect of zero-valent iron shavings. *International Journal of Hydrogen Energy*, **39**, 19331–19336.

9. Zhang, L., Zhang, L. and Li, D. (2015) Enhanced dark fermentative hydrogen production by zero-valent iron activated carbon micro-electrolysis. *International Journal of Hydrogen Energy*, **40(36)**, 12201–12208.

10. Noman, M., Yu, G., Elimian, E. A. and Yun, K. (2025) One step hydrothermal synthesis of green iron-modified catalyst by food waste digestate biogas residue for ozonation of ciprofloxacin: Characterization, degradation mechanism, DFT study and reactive oxygen species role. *Journal of Environmental Chemical Engineering*, **13(1)**.

11. Leroy-Freitas, D., Muñoz, R., Martínez-Mendoza, L. J., Martínez-Fraile, C. and García-Depraect, O. (2024) Enhancing Biohydrogen Production: The Role of Iron-Based Nanoparticles in Continuous Lactate-Driven Dark Fermentation of Powdered Cheese Whey. *Fermentation*, **10(6)**.

12. Pérez-Barragán, J., Martínez-Fraile, C., Muñoz, R., Vargas-Estrada, L., Maya-Yescas, R., León-Becerril, E., Castro-Muñoz, R. and García-Depraect, O. (2024) Iron (Magnetite) Nanoparticle-Assisted Dark Fermentation Process for Continuous Hydrogen Production from Rice Straw Hydrolysate. *Applied Sciences (Switzerland)*, **14(21)**.

13. Kumar, G., Mathimani, T., Rene, E. R. and Pugazhendhi, A. (2019) Application of nanotechnology in dark fermentation for enhanced biohydrogen production using inorganic nanoparticles. *International Journal of Hydrogen Energy*, **44(26)**.

14. Rafie, S. F., Sayahi, H., Abdollahi, H. and Abu-Zahra, N. (2023) Hydrothermal synthesis of Fe_3O_4 nanoparticles at different pHs and its effect on discoloration of methylene blue: Evaluation of alternatives by TOPSIS method. *Materials Today Communications*, **37**.

15. Ahmadi, H., Jalil, A., Khan, S., Phulpoto, I. A., Chengyu, Z. and Yu, Z. (2025) Novel supplementation of Fe_3O_4-doped green carbonized nanoparticles on hydrogenases genes and microbial biodiversity for enhancing biohydrogen yield in dark fermentation microbial electrohydrogenesis cells. *Journal of Industrial Microbiology and Biotechnology*, **52**.

16. Palanivel, P. D., Jovita, S. A., Babu, K. and Naina Mohamed, S. (2025) Harnessing dark fermentation: Mechanisms, metabolic pathways, and nanoparticle innovations for biohydrogen enhancement. *International Journal of Hydrogen Energy*, **109**.

17. Jamali, N. S., Md Jahim, J., Mumtaz, T. and Abdul, P. M. (2021) Dark fermentation of palm oil mill effluent by Caldicellulosiruptor saccharolyticus immobilized on activated carbon for thermophilic biohydrogen production. *Environmental Technology and Innovation*, **22**.

18. Mahmod, S. S., Jahim, J. M. and Abdul, P. M. (2017) Pretreatment conditions of palm oil mill effluent (POME) for thermophilic biohydrogen production by mixed culture. *International Journal of Hydrogen Energy*, **42(45)**, 27512–27522.

19. Yildirim, O. and Ozkaya, B. (2023) Effect of nanoparticles synthesized from green extracts on dark fermentative biohydrogen production. *Biomass and Bioenergy*, **170**.

20. Lakroun, S. E., Boutemak, K., Haddad, A., Rambabu, K., Hai, A., Lemaoui, T., Mettu, S. and Banat, F. (2025) Elevating hydrogen production efficiency in dark fermentation: The role of cobalt-doped magnetite nanoparticles with sugarcane molasses. *International Journal of Hydrogen Energy*, **124**.

21. Rana, S., Yadav, K. K., Sood, K., Ankush, Mehta, S. K. and Jha, M. (2020) Low Temperature Hydrothermal Method for Synthesis of Crystalline Fe_2O_3 and their Oxygen Evolution Performance. *Electroanalysis*, **32(11)**, 2528–2534.

22. Mishra, P., Thakur, S., Singh, L., Ab Wahid, Z. and Sakinah, M. (2016) Enhanced hydrogen production from palm oil mill effluent using two stage sequential dark and photo fermentation. *International Journal of Hydrogen Energy*, **41(41)**, 18431–18440.

23. O-Thong, S., Prasertsan, P., Intrasungkha, N., Dhamwichukorn, S. and Birkeland, N. K. (2007). Improvement of biohydrogen production and treatment efficiency on palm oil mill effluent with nutrient supplementation at thermophilic condition using an anaerobic sequencing batch reactor. *Enzyme and Microbial Technology*, **41(5)**.

24. Lin, R., Cheng, J., Ding, L., Song, W., Liu, M., Zhou, J. and Cen, K. (2016) Enhanced dark hydrogen fermentation by addition of ferric oxide nanoparticles using Enterobacter aerogenes. *Bioresource Technology*, **207**.

25. Zhang, J., Fan, C. and Zang, L. (2017) Improvement of hydrogen production from glucose by ferrous iron and biochar. *Bioresource Technology*, **245**.

26. Han, H., Cui, M., Wei, L., Yang, H. and Shen, J. (2011) Enhancement effect of hematite nano-particles on fermentative hydrogen production. *Bioresource Technology*, **102(17)**, 7903–7909.

27. Zhang, J., Fan, C., Zhang, H., Wang, Z., Zhang, J. and Song, M. (2018) Ferric oxide/carbon nanoparticles enhanced bio-hydrogen production from glucose. *International Journal of Hydrogen Energy*, **43(18)**, 8729–8738.

28. Jiang, X., Hu, J., Lieber, A. M., Jackan, C. S., Biffinger, J. C., Fitzgerald, L. A., Ringeisen, B. R. and Lieber, C. M. (2014) Nanoparticle facilitated extracellular electron transfer in microbial fuel cells. *Nano Letters*, **14(11)**.

29. Mohanraj, S., Kodhaiyolii, S., Rengasamy, M. and Pugalenthi, V. (2014) Phytosynthesized iron oxide nanoparticles and ferrous iron on fermentative hydrogen production using Enterobacter cloacae: Evaluation and comparison of the effects. *International Journal of Hydrogen Energy*, **39(23)**.

30. Zhao, X., Xing, D., Qi, N., Zhao, Y., Hu, X. and Ren, N. (2017) Deeply mechanism analysis of hydrogen production enhancement of Ethanoligenens harbinense by Fe^{2+} and Mg^{2+}: Monitoring at growth and transcription levels. *International Journal of Hydrogen Energy*, **42(31)**.

31. Lay, J. -J., Fan, K. -S., Hwang, J. -I., Chang, J. -I. and Hsu, P. -C. (2005) Factors Affecting Hydrogen Production from Food Wastes by Clostridium -Rich Composts. *Journal of Environmental Engineering*, **131(4)**.

32. Abdullah, M. F., Md Jahim, J., Abdul, P. M. and Mahmod, S. S. (2020) Effect of carbon/nitrogen ratio and ferric ion on the production of biohydrogen from palm oil mill effluent (POME). *Biocatalysis and Agricultural Biotechnology*, **23**.

33. Mishra, P., Thakur, S., Mahapatra, D. M., Wahid, Z. A., Liu, H. and Singh, L. (2018) Impacts of nano-metal oxides on hydrogen production in anaerobic digestion of palm oil mill effluent – A novel approach. *International Journal of Hydrogen Energy*, **43(5)**, 2666–2676.

34. Puranjan, M., Singh, L. and Zularisam, A. W. (2016) Influence of Nano Nickel Oxide (NNO) Particles on Hydrogen Production in Dark Fermentation of Palm Oil Mill Effluent. *Universiti Malaysia Pahang*.